



The transmission of intense transient and multiple frequency sound waves through orifice plates with mean fluid flow

A. Cummings, I.-J. Chang

► To cite this version:

A. Cummings, I.-J. Chang. The transmission of intense transient and multiple frequency sound waves through orifice plates with mean fluid flow. *Revue de Physique Appliquée*, 1986, 21 (2), pp.151-161. 10.1051/rphysap:01986002102015100 . jpa-00245420

HAL Id: jpa-00245420

<https://hal.science/jpa-00245420>

Submitted on 4 Feb 2008

HAL is a multi-disciplinary open access archive for the deposit and dissemination of scientific research documents, whether they are published or not. The documents may come from teaching and research institutions in France or abroad, or from public or private research centers.

L'archive ouverte pluridisciplinaire **HAL**, est destinée au dépôt et à la diffusion de documents scientifiques de niveau recherche, publiés ou non, émanant des établissements d'enseignement et de recherche français ou étrangers, des laboratoires publics ou privés.

Classification
 Physics Abstracts
 43.25

The transmission of intense transient and multiple frequency sound waves through orifice plates with mean fluid flow*

A. Cummings and I.-J. Chang

Department of Mechanical and Aerospace Engineering, University of Missouri-Rolla, Rolla, MO 65401, U.S.A.

(Reçu le 20 mai 1985, révisé le 25 octobre, accepté le 12 novembre 1985)

Résumé. — Nous présentons ici un modèle d'écoulement non visqueux, qui décrit la transmission des ondes sonores intenses à travers des tôles perforées avec écoulement moyen d'un fluide à travers les orifices, normal à la tôle. La dépendance en temps dans l'onde acoustique est arbitraire, et les équations différentielles qui régissent l'écoulement des orifices sont résolues dans le domaine temporel. Nous remarquons que la vitesse d'écoulement moyen et la perturbation de la vitesse du fluide dans l'orifice sont toutes les deux contenues dans un terme de résistance hydrodynamique dans les équations de base et que les pertes d'énergie acoustique dépendent de ces quantités. Nous comparons les prévisions théoriques de la transmission du son à travers les tôles perforées avec les données mesurées, et en général nous les trouvons toutes les deux en bon accord.

Abstract. — A inviscid flow model is presented here, describing the transmission of intense sound waves through perforated plates with mean fluid flow through the orifices, normal to the plate. The time dependence in the acoustic wave is arbitrary, and the differential equations governing the orifice flow are solved numerically in the time domain. It is noted that both the mean flow velocity and the orifice velocity perturbation are contained in a hydrodynamic resistance term in the governing equations, and that acoustic energy losses are dependent on these quantities. Comparison is made between theoretical predictions of sound transmission through orifice plates and measured data, and the agreement is found to be generally good.

1. Introduction.

There are several types of device, from « reactive » silencers in the exhaust systems of internal combustion (I.C.) engines to orifice flow meters in gas pipelines, in which intense sound waves are transmitted through perforated plates having mean fluid flow through the perforations. It is well known that both high acoustic amplitude and mean flow can independently bring about the conversion of acoustic energy into vortical energy, with subsequent dissipation of the sound energy into heat. This occurs because of the interaction between a superimposed sound field and a free shear layer, caused either by a high velocity acoustic flow (in the absence of a mean flow) or by a mean flow, separating upon encountering a sharp edge. This interaction also manifests itself in other transmission properties of the perforated structure, such as the acoustic impedance (in the case of periodic excitation). Sivian [1] was perhaps the first worker to note the

nonlinear impedance of orifices subjected to high amplitude sound fields in the absence of mean flow. Ingard and Ising [2] investigated both high amplitude acoustic impedance effects and mean flow effects at orifices, and found that high acoustic amplitude (with zero flow) and mean flow (at low acoustic amplitude) had similar effects in bringing about an increase in orifice resistance, over and above its linear, zero flow value. In the presence of both mean flow and high amplitude sound waves, however, the orifice flow field became rather more complicated, and different effects were noted in opposite flow half-cycles. A number of other workers have investigated the interaction between intense sound waves and orifices, more or less thoroughly. Hersch and Rogers [3], for example, gave a relatively detailed treatment of the acoustic impedance of orifices at low and high amplitudes with zero mean flow, and used a locally spherical inflow model that was an improvement on the parallel flow assumption made by certain other workers. In other work, investigators have concentrated on the acoustic energy loss mechanisms (as opposed to the impedance) involved in the interaction between a sound field and a

(*) This work was supported by the National Science Foundation under Research Grant MEA 8312399.

free shear layer. Bechert [4] and Howe [5], for example, reported significant experimental and theoretical studies (respectively) of this phenomenon.

In the majority of published works on acoustic interaction with sharp edges — with and without mean flow — it has been assumed that either the sound pressure or the particle velocity varied harmonically with time. Exceptions to this are a report by Rice [6] and a paper by Cummings [7], and in both of these pieces of work the differential equation governing the fluid flow in an orifice was solved numerically, for an arbitrary time variation of the forcing pressure. An experimental study of the transmission of high amplitude impulsive sound waves through duct terminations (nozzles and orifice plates) is reported by Salikuddin and Ahuja [8], and Cummings and Eversman [9] offered theoretical explanations of the observed acoustic energy deficit across the termination, though on the basis of a frequency-domain analysis.

Single frequency analyses of the interaction of intense sound waves with perforated structures have an inherent disadvantage : even in the presence of mean flow through the perforations, significant nonlinear effects can occur, producing harmonic distortion of (for example) a sinusoidal forcing pressure field. If the driving pressure were complex and periodic, then nonlinear inter-harmonic interaction effects would occur. In the case of a non-periodic (for example, transient or random) signal, then rather more complicated nonlinear effects take place. A frequency domain analysis cannot readily cope with these phenomena, but a numerical time domain (NTD) solution can be applied for any arbitrary time variation of the forcing pressure.

Accordingly, this paper deals with a time domain solution for the transmission of intense sound waves through a perforated plate with mean fluid flow through the perforations, travelling *normally* to the plate. The effects of both high acoustic particle velocity and of mean flow are incorporated into the theoretical model, and (as examples) both transient and complex periodic acoustic signals are examined. Comparison is made between the experimentally measured transmission properties of orifice plates under various flow conditions, and numerical predictions. Although details of the orifice flow field — such as ring vortices — are suppressed in the present model, other important features, for example the transfer of acoustic energy into vortical energy (with associated dissipation), and nonlinear and mean flow dependent impedance effects, are implicitly contained within the approach described here.

2. Theory.

In the absence of mean flow, the NTD method reported by Cummings [7] suffices to give good predictions of the acoustic transmission properties of perforated plates subjected to intense sound fields.

When mean flow is present, however, a somewhat modified approach must be taken, as follows. The fluid pressure and velocity in the neighbourhood of the perforated plate are split into a time-averaged component and an acoustic perturbation, respectively as

$$p = P + p', \quad (1a)$$

$$v = V + v', \quad (1b)$$

where the prime denotes the perturbation ; the velocity component of interest here is always that normal to the orifice plate and so the normal velocity may simply be written as $v = V + v'$, with an appropriate sign convention. It is necessary to use two distinct theoretical models for the sound transmission process : one where the velocity in the orifice is in the same direction as the time averaged velocity V , and the other where there is « reverse flow », and the orifice velocity opposes the direction of V .

Figure 1 shows the geometry of the system. For simplicity, the perforated plate is shown as being an orifice plate having a single hole (of area A_o), and located in a tube (which may be considered circular) of cross-sectional area A . This does not *have* to be the case, and multiple holes could be accommodated either by envisaging a multiply perforated plate in a tube or else by imagining a « bundle » of tubes, each containing a singly perforated plate, and replacing the tube walls (which would have to be of such a shape — for instance square — as to fit together) by stagnation stream tubes in an inviscid flow. The sign convention for velocity is positive for a left to right flow. The mean fluid flow goes from left to right, and it is assumed that a jet is formed by separation of the mean flow boundary layer, and that a *vena contracta* (of cross-sectional area A_{vc}) exists in the jet. Two locations are indicated, 1 before the mean flow streamlines converge on the orifice, and 2 at the *vena contracta*. In what follows, it is assumed that only the plane acoustic mode can propagate in the tube. It is further assumed that the sound source is at the upstream side of the orifice (since this would normally be the case in practice), though the opposite situation could easily be accommodated if necessary.

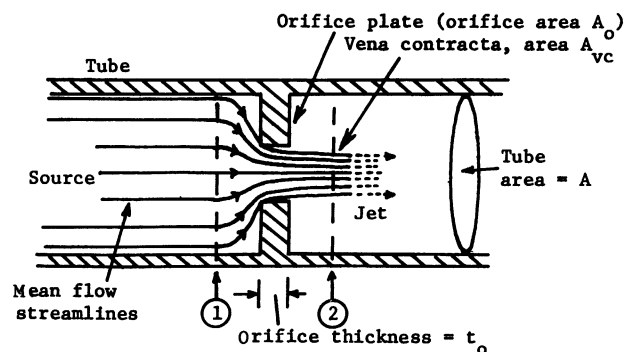


Fig. 1. — An orifice plate with mean flow.

2.1 POSITIVE ORIFICE FLOW. — The discussion diverges now into consideration of the separate models, as mentioned above. We first examine the case where the instantaneous orifice flow goes from left to right.

The object of the exercise here will be to find the pressure perturbation, p'_2 , at station 2, for a prescribed driving pressure p'_1 and for a prescribed geometry and mean flow speed in the orifice.

We ignore viscous effects in the theoretical development here, because of the relatively high Reynolds' numbers involved (typically at least 1 000, based on orifice diameter), and fluid viscosity is only implied inasmuch as boundary layer separation is assumed to take place at sharp edges. The hydrodynamic resistance, in the presence of either mean flow or high amplitude (or both), completely swamps the viscous resistance of the orifice. Bernoulli's equation may be written for streamlines between planes 1 and 2, in an unsteady in compressible flow,

$$p_2 - p_1 + \rho_0(v_2^2 - v_1^2)/2 + \rho_0 \partial(\phi_2 - \phi_1)/\partial t = 0, \quad (2)$$

the subscripts denoting position and ρ_0 , ϕ being the

fluid density and velocity potential ⁽¹⁾ respectively (we define $\mathbf{v} = \nabla\phi$). This equation is taken to describe the instantaneous hydrodynamic flowfield in and near the orifice. Provided the acoustic wavelength λ_0 is greater than about twice the width of the tube, the assumption of incompressibility is valid ⁽²⁾. If the mean and fluctuating flow components are taken to occupy the same region, then one may use the continuity equation to write

$$v_1 = v_2 \sigma C_c \quad (3a)$$

$$V_1 = V_2 \sigma C_c \quad (3b)$$

$$v'_1 = v'_2 \sigma C_c \quad (3c)$$

$$v_0 = v_2 C_c \quad (3d)$$

$$V_0 = V_2 C_c \quad (3e)$$

$$v'_0 = v'_2 C_c, \quad (3f)$$

where the subscript 0 refers to the orifice, σ (the fractional open area of the plate) is equal to A_0/A and C_c is a contraction coefficient, equal to A_{vc}/A_0 . Equations (3) may be combined with (2) to give

$$P_2 - P_1 + p'_2 - p'_1 + \rho_0(1 - \sigma^2 C_c^2)(V_0^2 + 2 V_0 v'_0 + v'_0 |v'_0|)/2 C_c^2 + \rho_0 \frac{\partial}{\partial t}(\phi_2 - \phi_1) = 0. \quad (4)$$

Taking the time average of (4) and subtracting it from equation (4) yields

$$p'_2 - p'_1 + \rho_0(1 - \sigma^2 C_c^2)(2 V_0 v'_0 + v'_0 |v'_0|)/2 C_c^2 + \rho_0 \frac{\partial}{\partial t}(\phi_2 - \phi_1) = \rho_0(1 - \sigma^2 C_c^2) \overline{v'_0 |v'_0|}/2 C_c^2, \quad (5)$$

the overbar denoting a time average. The third term on the left hand side of (5) is associated with a *resistive* pressure, brought about partly by the mean flow (the $2 V_0 v'_0$ term in parentheses) and partly by the fluctuating flow (the $v'_0 |v'_0|$ term) interacting with the velocity perturbation in the orifice. We note that the nonlinear resistance term contains $|v'_0|$ rather than v'_0 , to ensure that the term has the correct sign as v'_0 varies between positive and negative values. The fourth term on the left hand side of (5) represents a *reactive* pressure associated with the « attached mass » of the orifice; physically, this is caused by the concentration of acoustic kinetic energy in and around the orifice. The reactive pressure may alternatively

be expressed as $\rho_0 l \dot{v}'_0$, where l is the « mass end correction » of the orifice ⁽³⁾.

It is now necessary to relate p'_2 to the orifice velocity perturbation v'_0 . The control volume shown in figure 2 is utilized here. It is assumed that the mean fluid flow forms a uniform jet as shown, surrounded by stationary fluid. Then the acoustic pressures and particle velocities in regions 3 and 4 may be related as follows

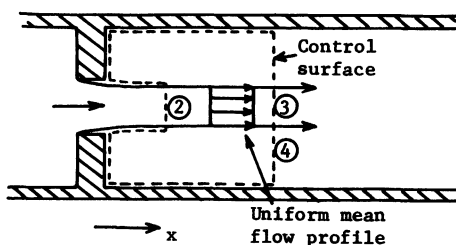


Fig. 2. — The control volume for downstream radiation.

⁽¹⁾ Velocity potential does not, of course, exist in a rotational flow and ϕ_2 is assumed to be defined only in the jet core where the vorticity may reasonably be put to zero.

⁽²⁾ Exclusively plane wave propagation in the tube is assured, and λ_0 is much greater than the orifice dimensions, so the velocity field near the orifice is all of the same phase. As long as the acoustic density fluctuations are small compared to the mean fluid density, the flow is then essentially incompressible.

⁽³⁾ The term $\partial(\phi_2 - \phi_1)/\partial t$ is equal to $\int_1^2 (\partial V_s/\partial t) ds$,

V_s being the fluid velocity in streamline coordinates and s the direction along the streamline. If the attached mass of fluid in and around the orifice is assumed to vibrate like an equivalent uniform plug of length l , containing all of the kinetic energy in and near the orifice, then the above integral is clearly equal to $l \partial V_s/\partial t$, that is, $l \dot{v}'_0$.

[10], if no acoustic reflection takes place to the right of the orifice plate :

$$v'_3 = K p'_3 / \rho_0 c_0 (1 - MK) \quad (6a)$$

$$v'_4 = K p'_4 / \rho_0 c_0 = K p'_3 / \rho_0 c_0, \quad (6b)$$

if $p'_4 = p'_3$ (which was shown to be approximately true in reference [10], even for quite high subsonic Mach numbers); here c_0 is the speed of sound, M is the mean flow Mach number in the jet, $= V_2/c_0$. The quantity K is equal to c_x/c_0 , where c_x is the propagation speed of the *coupled* wave system in the jet flow and in the surrounding stagnant fluid (x is the axial coordinate; see Fig. 2). To find K , one should solve an eigen-equation involving Bessel functions (if the tube is circular) [10], but here we may use a simpler interpolation formula, as follows. Define $\eta = \sigma C_c$; then if $\eta \rightarrow 0$, $K = 1$ (corresponding to an infinitesimally narrow jet), whereas if $\eta \rightarrow 1$, $K = 1/(1 + M)$ (corresponding to a jet that fills the whole tube). Then we may write an interpolation formula

$$K = 1/(1 + \eta M). \quad (7)$$

Cummings and Haddad [11] investigated the entropy fluctuations occurring when a sound wave is transmitted through a sudden area expansion in a pipe containing mean fluid flow, and showed that these are actually very small, so pressure and density fluctuations may be related isentropically, to good accuracy. Thus

$$p' = \rho' c_0^2, \quad (8)$$

where ρ' is the density perturbation.

The quasi-steady continuity and momentum equations in the perturbed pressure, density and velocity, for the control volume, are now linearized (because we assume the acoustic field away from the orifice to be linear). If the pressure perturbation over the entire left hand side of the control volume is equal to p'_2 (this assumption is reasonable on the basis of parallel streamlines, and also has extensive experimental justification), then the linearized equations may be combined to give the simultaneous equations

$$\alpha_1 p'_2 + \beta_1 v'_2 = \gamma_1 p'_3, \quad (9a)$$

$$\alpha_2 p'_2 + \beta_2 v'_2 = \gamma_2 p'_3, \quad (9b)$$

where

$$\alpha_1 = M C_c \sigma \quad (10a)$$

$$\beta_1 = \rho_0 c_0 C_c \sigma \quad (10b)$$

$$\gamma_1 = K + M(1 - MK + K^2) C_c \sigma / (1 - MK) \quad (10c)$$

$$\alpha_2 = 1 + M^2 \sigma C_c \quad (10d)$$

$$\beta_2 = 2 \rho_0 c_0 M C_c \sigma \quad (10e)$$

$$\gamma_2 = 1 + M(M - M^2 K + 2 K) C_c \sigma / (1 - MK). \quad (10f)$$

Equations (9a, b) and (3f) now yield

$$p'_2 = v'_0 F, \quad (11a)$$

where

$$F = -(\beta_1 \gamma_2 - \beta_2 \gamma_1) / C_c (\alpha_1 \gamma_2 - \alpha_2 \gamma_1). \quad (11b)$$

We may now write (5) as a differential equation in v'_0 by substituting $\rho_0 l \dot{v}'_0$ for the reactive pressure and utilizing equation (11a),

$$[\rho_0 l] \dot{v}'_0 + \{ \rho_0 (1 - \sigma^2 C_c^2) (2 V_0 + |v'_0|) / 2 C_c^2 + F \} v'_0 = p'_1 + \rho_0 (1 - \sigma^2 C_c^2) \overline{v'_0 |v'_0|} / 2 C_c^2. \quad (12)$$

Provided appropriate values of l and C_c can be chosen, equation (12) may be solved numerically for an arbitrary time-variation of p'_1 . The transmitted pressure p'_2 may then be found from (11a). The second term on the right hand side of (12) appears to present a problem, but its value may be found by iteration. Initially this term is put equal to zero, and the equation is solved. Then the values of v'_0 so obtained are used to find a new value for the term. The equation is solved again, and so on, until the process converges. Further discussion of the role of the time averaged term will be postponed until section 4.

Equations (6a, b) are, of course, only valid for a reflection-free termination. In any other situation, appropriate alternative expressions would have to be employed.

2.2 NEGATIVE ORIFICE FLOW. — The case considered here is where flow reversal occurs, and $-v'_0 > V_0$. It is assumed that the reverse orifice flow separates, forming a jet that is directed to the left (we refer to Fig. 1). We further assume that a *vena contracta*, of area A_{vc} , is formed in this jet. Now the velocity perturbation v'_2 may be taken to be uniform across the pipe (since plane 2 is temporarily on the upstream side of the orifice), whereas the mean flow is still that shown in figure 1; the mean flow contraction coefficient C_{∞} may be put equal to a typical value of 0.61 in this case. Then, the continuity equation leads to the relationships

$$V_1 = V_2 \sigma C_{\infty} \quad (13a)$$

$$v'_2 = v'_1 \sigma C_c \quad (13b)$$

$$V_0 = V_2 C_{\infty} \quad (13c)$$

$$v'_2 = v'_0 \sigma. \quad (13d)$$

Equations (13a-d) may be combined with (2) to give the equivalent of equation (4). The time average of this is taken and subtracted from the equation itself. Equation (11a) still describes the downstream radiation (since the mean jet flow still exists, albeit in a briefly interrupted form), and finally an equation of motion may be written down,

$$[\rho_0 l] \dot{v}'_0 + \{ \rho_0 \sigma V_0 (1/C_{\infty} - 1/C_c) + \rho_0 (1 - \sigma^2 C_c^2) |v'_0| / 2 C_c^2 + F \} v'_0 = p'_1 + \overline{v'_0 |v'_0|} \rho_0 (\sigma^2 - 1/C_c^2) / 2. \quad (14)$$

As was the case with equation (12), equation (14) may be solved if values of l and C_c can be specified. We note that if $C_c \simeq C_{\infty}$ (as would normally be the case), the resistive term arising from the mean flow is almost completely suppressed here. This is in sharp contrast with equation (12).

Despite the various complications involved with equations (12) and (14), the *sine qua non* of the physical process is that the fall in pressure as the fluid accelerates to pass through the orifice, together with the fact that « pressure recovery » of the fluid outflow does *not* occur (because of the flow separation at the orifice), brings about a hydrodynamic resistance in the orifice transmission process. The energy absorption mechanism associated with this resistance is the conversion of acoustic energy into vortical energy *via* the interaction of the acoustic flow with the free shear layer in the orifice outflow.

2.3 NUMERICAL SOLUTION TO EQUATIONS OF MOTION. —

The fourth order Runge-Kutta method was used to solve equations (12) and (14) in the time domain. The forcing pressure p_1 was either transient, or complex and periodic, but began from zero at a given time. Thus the signal was « switched on » at that time. In the Runge-Kutta scheme, an initial value of v'_0 is required, and the causality requirement dictated that v'_0 should be zero at the switching on time, when p'_1 was also zero.

In the case of transient signals, p'_1 versus time t was specified over the duration of the signal, and the solution was allowed to proceed until the transmitted pressure had settled almost to zero.

With complex periodic signals, p'_1 versus t for a single cycle was specified, beginning at a time when $p'_1 = 0$. The signal was switched on at the beginning of a cycle, and then p'_1 was made to go through a series of additional, identical, cycles. A steady-state solution for the transmitted pressure was reached after several cycles, and it was found that the solution had always reached a steady state by the seventh cycle, which was then taken as being representative.

As well as the transmitted pressure-time history, the spectrum of p'_2 is of interest, and this was found by a fast Fourier transform (FFT) routine, and expressed either as a discrete Fourier transform, in the case of a transient signal, or as a Fourier series in the case of a complex periodic signal.

During the Runge-Kutta integration process, equation (12) was taken as the governing differential equation whenever $-v'_0 < V_0$. If $-v'_0 \geq V_0$, equation (14) was solved. These inequalities were monitored at each integration step and appropriate action taken.

The mass end correction l merits brief mention here. In the absence of mean flow, l would be given (see for example the paper by Ingard [12]) by the expression

$$l = 0.85 D_0 + t_0, \quad (15)$$

D_0 being the orifice diameter and t_0 the orifice thick-

ness. When mean flow through the orifice occurs, normal to the plate, the rotational nature of the flow on the outflow side of the orifice effectively removes the attached mass in this region. Within the orifice, one may expect some reduction in the inertance, though insufficient data are available for one to determine exactly how much. As a compromise, we assume that a 50 % reduction occurs, and therefore

$$l = 0.85 R_0 + t_0/2, \quad (16)$$

R_0 being the orifice radius. This latter expression was used here to find l . Any inaccuracies in this estimate of l would be totally swamped by the large orifice resistance, caused by the mean flow and possibly also by the nonlinear hydrodynamic resistance. In the case of intense sound transmission through an orifice with no mean flow, Cummings [7] was able to calculate l at each integration step as the solution proceeded, from an empirical formula relating l to the volume of the vortical fluid in and around the orifice, but no such procedure is possible where mean flow is present and neither, we feel, is it necessary.

It was found that the contraction coefficient C_c was dependent on v'_0/V_0 , and that this dependence was different in the positive and negative flow half-cycles. In section 3, the development of empirical expressions for C_c is described.

In the case of multiple orifices, little modification to the foregoing theory is necessary provided the orifices are sufficiently far apart that interaction effects between adjacent orifice flows can be neglected. We simply replace the orifice area A_0 by NA_0 , where N is the number of orifices and A_0 is the area of each orifice.

3. Empirical determination of the orifice contraction coefficient.

In the course of this investigation, the values of C_c were adjusted so as to give the best agreement between the measured and predicted values of p'_2 . It was found that (i) different optimum values of C_c were obtained for positive and negative flow half-cycles (« positive » and « negative » referring to the sign of v'_0), and (ii) the optimum value of C_c was dependent on the peak value of v'_0 in each half-cycle.

One could, perhaps, allow C_c to vary continuously during the orifice flow cycle (this term being used — rather loosely — here to apply to transient as well as periodic signals), as a function of some appropriate parameter, but it was considered to be sufficient to use constant values during the positive and negative half-cycles, determined by the peak values of v'_0 in the positive and negative directions, denoted \hat{v}'_{0+} and \hat{v}'_{0-} respectively (\hat{v}'_{0-} being a *positive* quantity). It was, moreover, considered that $\zeta_+ = \hat{v}'_{0+}/V_0$ and $\zeta_- = \hat{v}'_{0-}/V_0$ would be the determining parameters of C_{c+} and C_{c-} (the values appropriate to the positive and negative half-cycles respectively). It seemed reasonable

to expect C_c to be dependent on the magnitude of the orifice velocity perturbation as a function of the mean flow velocity, rather than in absolute terms. For example, at the onset of reverse flow, $\zeta_- = 1$, and one might perhaps expect C_{c-} to behave in an unusual manner for values of ζ_- close to unity. For small values of both ζ_+ and ζ_- , values of C_{c+} and C_{c-} corresponding to steady flow could be expected, since the mean jet flow would be only slightly perturbed, by the acoustic wave. A typical steady-flow value of C_c is 0.61, if $\sigma \ll 1$. Conversely, with zero mean flow, for sound fields of at least moderate intensity, one would expect C_c to take on an appropriate value. Cummings [7] found that $C_c = 0.75$ gave good results in this situation, so as both ζ_+ and ζ_- tend to infinity, then C_{c+} and C_{c-} should tend toward a value of 0.75.

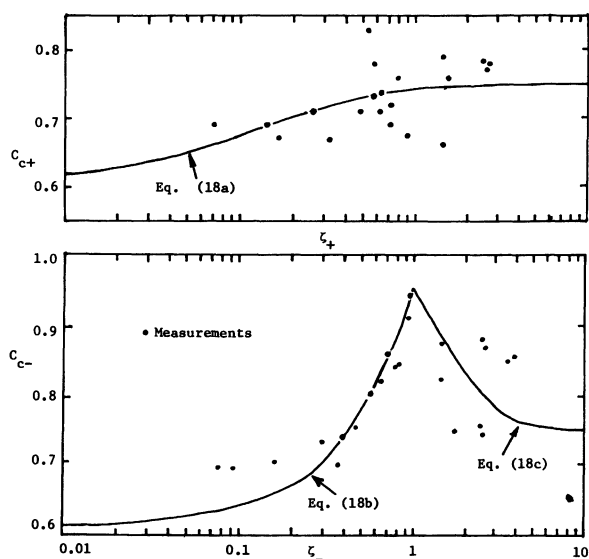


Fig. 3. — Contraction coefficients versus peak velocity parameter.

A series of experimental tests was carried out on a sharp-edged orifice of 6.35 mm diameter using transient signals, in which ζ_+ and ζ_- were varied both by varying the peak values of p'_1 and by varying V_0 . Optimum values of C_{c+} and C_{c-} , as functions of ζ_+ and ζ_- respectively, were determined. Figure 3 shows the results of these tests, together with empirical expressions intended to give a « best fit » to the measured data as well as the desired behaviour as $\zeta_{+,-} \rightarrow 0$ and $\zeta_{+,-} \rightarrow \infty$. A quantity ε_+ is defined as

$$\varepsilon_+ = (C_{c+} - 0.61)/0.14 \quad (17a)$$

and a quantity ε_- is defined,

$$\varepsilon_- = (C_{c-} - 0.61)/0.34, \quad \zeta_- \leq 1 \quad (17b)$$

$$\varepsilon_- = (C_{c-} - 0.75)/0.2, \quad \zeta_- > 1. \quad (17c)$$

The empirical expressions for $\varepsilon_{+,-}$ are :

$$\varepsilon_+ = 1 - 1/(1 + 13 \zeta_+^{1.176}), \quad (18a)$$

$$\varepsilon_- = \zeta_-^{1.05}, \quad \zeta_- \leq 1 \quad (18b)$$

$$\varepsilon_- = \exp[-0.83(\zeta_- - 1)], \quad \zeta_- > 1. \quad (18c)$$

It can be seen that there is some degree of scatter in the experimental data, as one would expect, but there are definite trends. For positive flow, C_{c+} varies more or less monotonically over the range of ζ_+ , with apparently random variation in the measured data. This is to be expected, on the basis of physical arguments, since no dramatic change in behaviour would be expected as ζ_+ is varied. On the other hand, C_{c-} might be expected to exhibit different behaviour for $\zeta_- < 1$ and $\zeta_- > 1$, and this appears to be the case. A peak value of C_{c-} of about 0.95 is noted when $\zeta_- = 1$, with a rather gradual falling-off on either side of the peak.

In the implementation of equations (18a-c) in the NTD solution scheme, an iterative procedure was used. To start with, values of $C_{c+} = 0.7$ and $C_{c-} = 0.75$ were used. The solution was run once, and values of ζ_+ and ζ_- were found from the calculated maximum and minimum values of v'_0 . New values of C_{c+} and C_{c-} were found from the empirical formulae and the solution was run once more. This process was repeated three times, at which point convergence invariably occurred.

4. The role of the constant term in the forcing function.

In equations (12) and (14), a constant term appears, involving the mean of the orifice velocity perturbation multiplied by its absolute value. Physically, this represents an additional time-averaged pressure differential across the orifice, brought about by nonlinear « rectification » of the orifice velocity perturbation. This pressure is grouped together with the forcing pressure p'_1 . As previously mentioned, this term may be incorporated in the solution by using an iterative procedure. The question arises : is it strictly necessary to include this term, since it merely represents a D.C. forcing pressure, and what effect will discarding it have on the solution ? The answer is not immediately obvious, as it would have been in the case of linear governing equations.

In the case of a transient pressure signal, it is quite clear that $\overline{v'_0 | v'_0|} \rightarrow 0$ as the averaging time tends to infinity, which in the present context signifies that there is no time for a steady additional pressure differential across the orifice to be built up, during the time history of the signal.

In the case of a continuous signal, the situation is less clear. Some numerical studies were carried out, with the object of gauging the importance of the constant forcing term, and assessing whether it could reasonably be neglected. Figure 4 shows a typical result, for $D_0 = 6.35$ mm, $t_0 = 0$, $V_0 = 28$ m/s, pipe diameter =

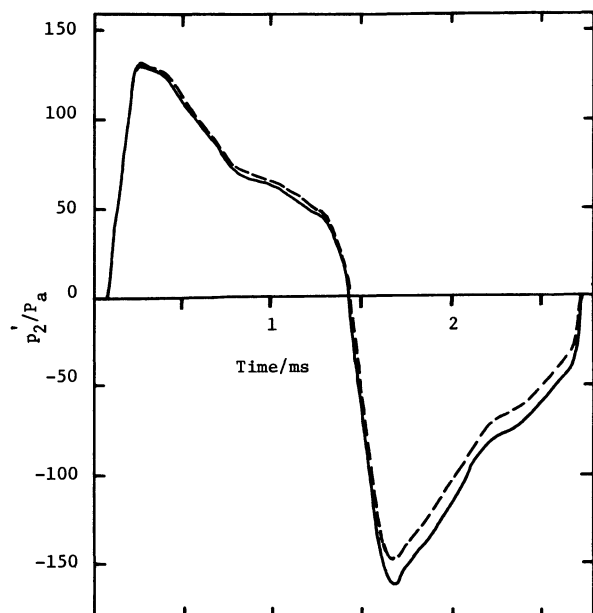


Fig. 4. — Sample calculations of p'_2 , with and without the constant term in p'_1 ; —, constant term included; — — —, constant term not included.

50.5 mm, $\rho_0 = 1.2 \text{ kg/m}^3$, $c_0 = 344 \text{ m/s}$; the time variation of p'_1 is that shown in figure 12. The dashed curve in figure 4 is one cycle of p'_2 without the constant term included, and in the solid curve, the constant term has been incorporated. It can be seen that the two curves of p'_2 are closely similar, though the curve with the constant term included is shifted downward on average by about 5 % of the positive peak pressure in p'_2 . The constant term in the forcing pressure is -42 Pa , that is, about 2.3 % of the positive peak value of p'_1 . Thus, even though the governing differential equations of the system are nonlinear, it appears that the constant term in the forcing pressure brings about principally a D.C. shift in the transmitted pressure, with very little change in the A.C. signal component. In the other cases studied, similar conclusions were reached. Indeed, the theoretical results presented in reference [7], for the transmission of intense sound through orifices in the absence of mean flow, were obtained by completely neglecting the constant term in the forcing pressure. Even so, excellent agreement was obtained between the predicted and measured transmission properties of orifices for periodic signals. A salient point here is that the measuring microphone could not detect the D.C. component of the signals.

In view of the above comments, it was decided to discard the constant term in the forcing pressure, in equations (12) and (14).

5. Measurements.

The arrangement by which experimental tests were conducted is illustrated in figure 5. An orifice plate was mounted between flanges in a 50.5 mm internal

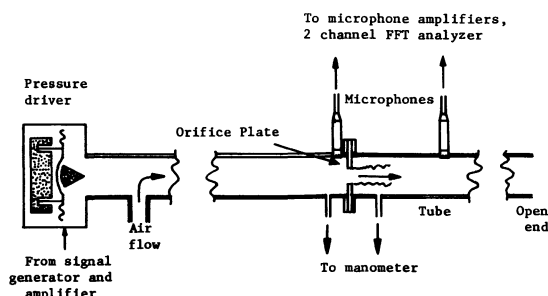


Fig. 5. — The measurement apparatus.

diameter pipe. Air from a silenced supply was fed into the pipe by means of a side branch, and a « pressure » driver supplied the acoustical signal. The driver was connected to a power amplifier and a signal generator, which was made to produce transient signals consisting of half a cycle of a square wave, or else bursts of a square wave signal. These square wave signals were not, of course, accurately reproduced by the driver, but the actual resultant acoustical signals were of suitably « broadband » frequency content for the purpose : the transient signals contained both rapid and more gradual pressure changes, and the signal bursts (or rather, their steady signal equivalents) were rich in harmonics. These features were, we felt, desirable in order to test the theory and computational scheme to the full. The advantage of using short-duration signals was that the effects of axial wave reflections could be eliminated by sampling the signal before the first reflection arrived.

The orifice plate itself was utilized as a meter for the mean flow, and two narrow static pressure tapings were drilled in the pipe wall upstream and downstream (at the appropriate positions) of the flanges, a U-tube manometer being used to register the pressure differential. Condenser microphones of 6.4 mm diameter were used to detect the acoustical signal, and their outputs were fed to a two-channel microphone amplifier and then to a two-channel FFT analyser and digital plotter. The tube termination at the downstream side of the orifice plate was left open to accommodate the air flow.

Several orifice plates were tested, including 6.4 mm and 12.7 mm diameter sharp-edged single orifices, a square-edged orifice of 6.6 mm diameter and thickness 3.2 mm, and a five-hole orifice plate with orifice diameter 6.6 mm and thickness 3.2 mm.

6. Comparisons between experiment and theory.

A wide variety of possible combinations of parameters was investigated : low mean flow with intense sound, low mean flow with less intense sound, higher mean flow with intense sound, *et cetera* (the zero flow case is not reported here, having been discussed at length by Cummings [7]); and, of course, single hole and multi-hole orifice plates were examined, as well as the effect of

differing orifice diameters; both short-duration transient signals and bursts of periodic signal were also utilized. We discuss only representative cases here.

In figure 6, a comparison is made between the predicted and measured $p'_2 - t$ histories for a single 6.4 mm diameter sharp-edged orifice with a fairly high value of V_0 (48.4 m/s, corresponding to a Mach number of 0.14) and a high pressure transient signal. Good agreement is observed between prediction and measurement. The predicted and measured spectra (in the form of the modulus of the discrete Fourier transform, $|P'_2(f_k)|$) of p'_2 are also compared, and satisfactory agreement is noted here, too. Figure 7 shows data on the same orifice for a transient signal, with the same value of V_0 , but at a lower sound pressure. Again, there is good agreement between the predicted and measured transmitted pressure. We may see that nonlinear

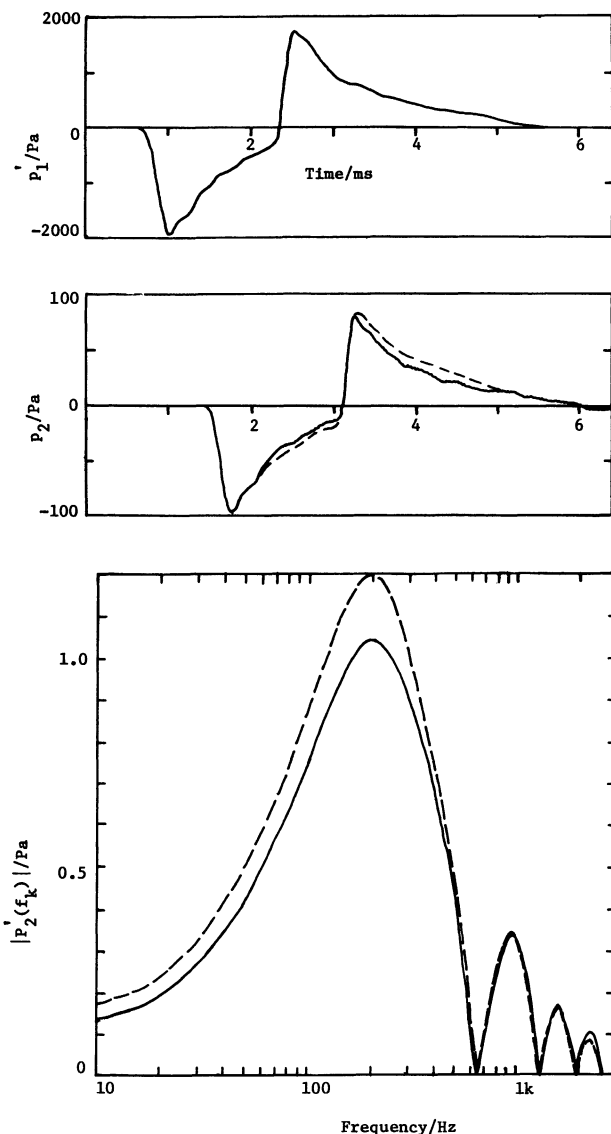


Fig. 6. — Transmission characteristics of 6.4 mm diameter sharp-edged orifice, $V_0 = 48.9$ m/s; —, experimental; — — —, theoretical.

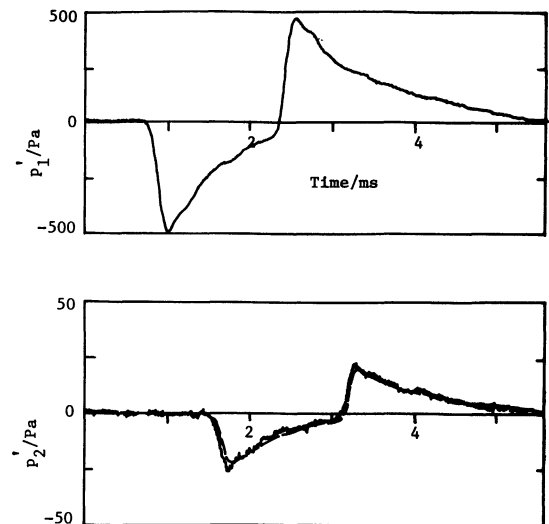


Fig. 7. — Transmission characteristics of 6.4 mm diameter sharp-edged orifice, $V_0 = 48.9$ m/s; —, experimental; — — —, theoretical.

effects here are small: the ratio between the measured negative peak values of p'_1 and p'_2 in each of the two cases is about 20.5, with the ratio between corresponding positive peak values being about 21.4. In passing we note the presence of a certain degree of flow noise superimposed on the transmitted pressure signal.

Figures 8 and 9 show data on p'_1 and p'_2 (again, both predicted and measured), for the 6.4 mm sharp-edged orifice with a lower value of V_0 (19.9 m/s corresponding to a Mach number of 0.057), at higher and lower sound pressures respectively, for a transient signal. We note that the transmitted pressure is quite accurately predicted in both cases. There are two further features to be noted in the comparison. First, the ratio between the peak negative values of p'_1 and p'_2 in each of the two cases is much smaller than the ratios in figures 6 and 7; the same is true of the ratio of peak positive values. This is because of the lower mean flow speed in figures 8 and 9; a smaller orifice resistance brings about a greater pressure transmission coefficient. The second point is that nonlinear effects are more noticeable here because of the lower mean flow speed. The ratio between the peak negative values of p'_1 and p'_2 in figure 8 is 8.5, but is only 6.3 in figure 9. The ratio between the peak positive values of p'_1 and p'_2 in figure 8 is 15.3, and is 11.2 in figure 9. There is clearly much more variation here between these pressure transmission ratios than there is in the case of the data shown in figures 6 and 7, and this is because the data in figures 8 and 9 correspond to situations where flow reversal occurs during the negative flow half-cycle. For example, the predicted negative peak value of v'_0 in figure 9 is -31.6 m/s, whereas $V_0 = 19.9$ m/s.

In figure 10, the predicted and measured transmitted pressures are shown for a transient wave of fairly high pressure impinging on a 12.7 mm diameter sharp-

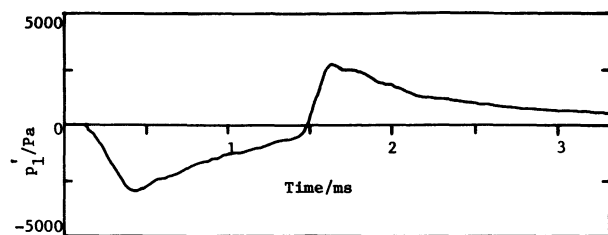


Fig. 8. — Transmission characteristics of 6.4 mm diameter sharp-edged orifice, $V_0 = 19.9$ m/s; —, experimental; — — —, theoretical.

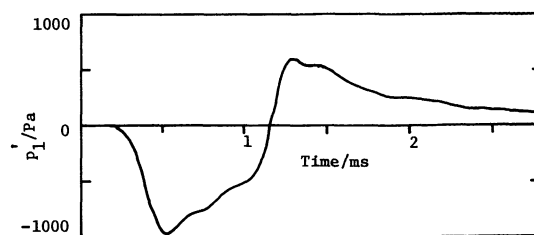


Fig. 10. — Transmission characteristics of 12.7 mm diameter sharp-edged orifice, $V_0 = 48$ m/s; —, experimental; — — —, theoretical.

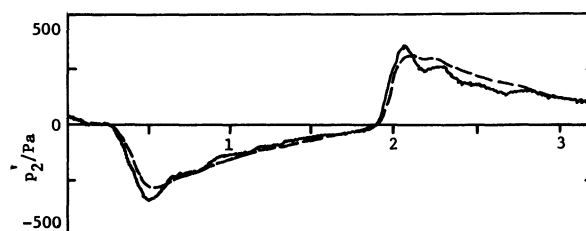
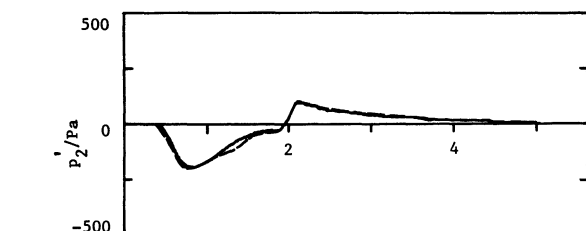
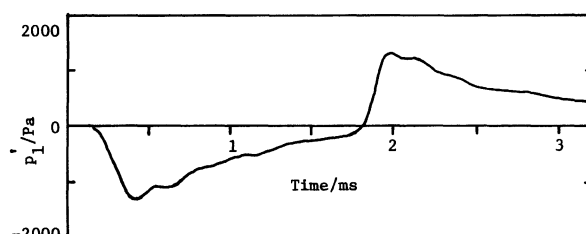
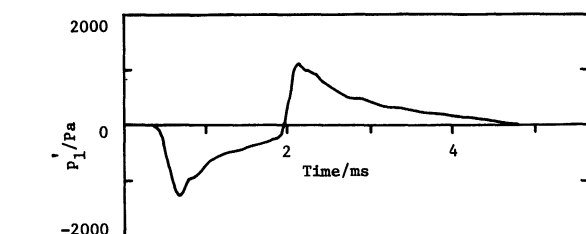
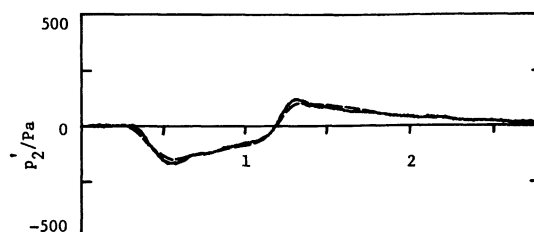
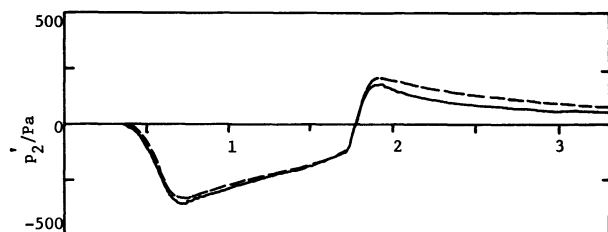


Fig. 9. — Transmission characteristics of 6.4 mm diameter sharp-edged orifice, $V_0 = 19.9$ m/s; —, experimental; — — —, theoretical.

Fig. 11. — Transmission characteristics of five-hole orifice plate (thickness = 3.2 mm) with 6.6 mm diameter square-edged orifices, $V_0 = 46.2$ m/s; —, experimental; — — —, theoretical.

edged orifice, with $V_0 = 48$ m/s. Good agreement between the predicted and measured time histories of p'_2 may be noted. The transmitted pressure is higher here, compared to the incident pressure — because of the larger orifice area — than it would have been in the case of the 6.4 mm orifice under the same conditions. A comparison may be made with the data shown in figure 7; although the peak incident pressure there is only about half that of the data in figure 10, the comparison is still valid because nonlinear effects are fairly small in both cases.

A comparison is made, in figure 11, between the predicted and measured transmitted pressures for a fairly high pressure transient wave impinging on an

orifice plate 3.2 mm thick, having five square-edged holes of 6.6 mm diameter, with $V_0 = 46.2$ m/s. Four of the holes were at the corners of a square of side 21 mm, and the fifth hole was at the centre. The square-edged geometry brought about considerably greater flow noise than that produced by the sharp-edged orifices, and this noise is superimposed on the p'_2 time history. Good agreement between experiment and theory is still observed in this case, however, and even though the holes are fairly closely spaced, inter-orifice interaction would seem to be small.

Figure 12 shows the predicted and measured transmitted pressures for a fairly intense periodic signal burst

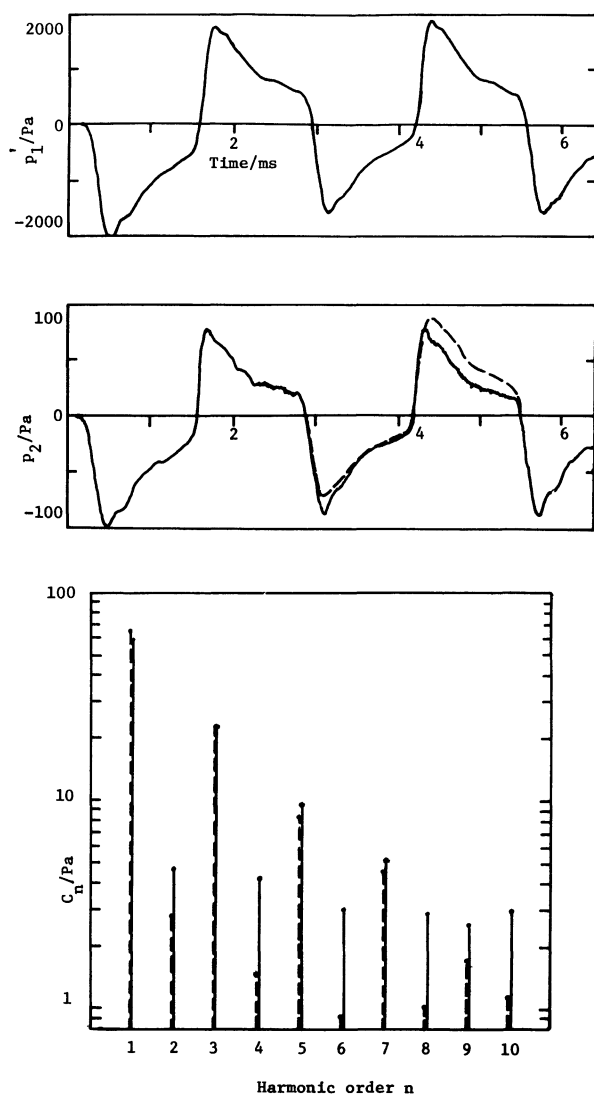


Fig. 12. — Transmission characteristics of 6.4 mm diameter sharp-edged orifice, $V_0 = 48.9$ m/s, for a signal burst; —, experimental; — — —, theoretical.

interacting with a 6.4 mm diameter sharp-edged orifice with $V_0 = 48.9$ m/s. There is a small D.C. discrepancy between the theoretical and measured time histories of p'_2 but otherwise the agreement is good. (This discrepancy cannot be explained by the constant term in the forcing pressure, which makes virtually no difference to the predictions in this particular case, even in the D.C. component of p'_2). A comparison is also made between the predicted and measured spectra of p'_2 , in the form of the amplitudes, C_n , of the first ten terms (excluding the constant term) in the Fourier series for the equivalent continuous signal. Odd terms dominate the series, and the predicted and measured values of these terms are in good agreement. Agreement between the predicted and measured values of the even terms is less good, but this is not of great significance in view of the minor role of these terms.

Although the formulae representing the coefficients used in the predictions described here were obtained

empirically, they produced universally good agreement between predictions and measurements in the present series of tests, over a range of flow speeds, acoustic pressures and orifice diameters. It is therefore felt that the comparisons are valid and that the expressions for the contraction coefficients used should be more generally applicable.

7. Discussion.

The results presented in this paper have demonstrated that it is possible to provide an accurate description of intense acoustic transmission through perforated plates with normal mean fluid flow, on the basis of a fairly simple inviscid flow model that embodies the essential features of the phenomenon. The model also permits an arbitrary time variation in the field variables. Both mean flow and large acoustic velocity perturbations are seen to bring about an increase in the orifice resistance; this appears to be the principal effect, and the orifice reactance would seem to play a relatively minor role in the transmission mechanism. The point at which nonlinear effects become noticeable varies with mean flow speed and is best expressed in terms of orifice velocity perturbation amplitude (for a sinusoidal signal). For zero flow, nonlinear effects typically become important when the amplitude is greater than about 0.5 – 1 m/s (this depending on geometry and frequency), and in the presence of flow, when the amplitude is greater than the mean flow speed in the orifice.

It proved to be necessary to allow the orifice contraction coefficient to depend on the magnitude of the acoustic velocity perturbation in the orifice, as a fraction of the mean flow velocity. Special provision had to be made for the situation where «flow reversal» in the orifice occurred but the empirical expressions for the contraction coefficient seemed to give fairly satisfactory results. It would, no doubt, be possible to devise an improved means of calculating the contraction coefficient, though any great complication in this process would hardly be justifiable in a theoretical model of this type.

There are of course other configurations, involving mean flow and perforated plates, that are of practical interest. For example, the situation where there is tangential mean flow on one side of the plate can occur in I.C. engine silencers and also in the perforated attenuating liners which are used in jet aircraft engines. Another case, that can be of importance in I.C. engine silencers, is that in which there is tangential mean flow across *both* sides of the perforated plate, perhaps also with some degree of flow through the perforations. These cases would, of course, have to be examined separately. The work of Rogers and Hersh [13], on the effect of grazing flow on the steady flow resistance of perforated plates, could perhaps be of use in these investigations.

The model described here should yield a reasonably accurate quantitative description of the *local* acoustic transmission properties of perforated plates under the specified flow conditions. In a particular application, perhaps involving cavities or tubes bounded in part by perforated walls, the model would furnish boundary

conditions, which should be matched up to the sound field in the enclosure by some appropriate means. To retain the generality of the method for an arbitrary time-dependence of the acoustic signal, an overall NTD solution method would probably be advantageous.

References

- [1] SIVIAN, L. J., *J. Acoust. Soc. Am.* **7** (1935) 94.
 - [2] INGARD, U. and ISING, H., *J. Acoust. Soc. Am.* **42** (1967) 6.
 - [3] HERSH, A. S. and ROGERS, T., *Am. Inst. of Aeronautics and Astronautics 2nd Aeroacoustics Conference* (1975), paper 75-495.
 - [4] BECHERT, D. W., *Am. Inst. of Aeronautics and Astronautics 5th Aeroacoustics Conference* (1979), paper 79-0575.
 - [5] HOWE, M. S., *J. Fluid Mech.* **91** (1979) 209.
 - [6] RICE, E. J., *N.A.S.A. Tech. Memo TM X-67950* (1971).
 - [7] CUMMINGS, A., *Am. Inst. of Aeronautics and Astronautics 9th Aeroacoustics Conference* (1984), paper 84-2311.
 - [8] SALIKUDDIN, M. and AHUJA, K. K., *J. Sound Vib.* **91** (1983) 479.
 - [9] CUMMINGS, A. and EVERSMAN, W., *J. Sound Vib.* **91** (1983) 503.
 - [10] CUMMINGS, A., *J. Sound Vib.* **38** (1975) 149.
 - [11] CUMMINGS, A. and HADDAD, H., *J. Sound Vib.* **54** (1977) 611.
 - [12] INGARD, U., *J. Acoust. Soc. Am.* **25** (1953) 1037.
 - [13] ROGERS, T. and HERSH, A. S., *Am. Inst. of Aeronautics and Astronautics 2nd Aeroacoustics Conference* (1975), p. 75-493.
-